



Nanolithography based on an atom pinhole camera for fabrication of metamaterials

P.N. Melentiev^{a,*}, A.V. Zablotskiy^b, A.A. Kuzin^b, D.A. Lapshin^a,
A.S. Baturin^b, V.I. Balykin^a

^a *Institute of Spectroscopy, Russian Academy of Sciences, 142190 Troitsk, Moscow reg., Russia*

^b *Moscow Institute of Physics and Technology, Dolgoprudny, Moscow reg., Russia*

Received 10 April 2009; received in revised form 31 July 2009; accepted 11 August 2009

Abstract

We have experimentally realized a method of images construction in atom optics, based on the idea of optical pinhole camera. Generation of identical images with maximum resolution has been explored. With the use of an atom pinhole camera we have built on a Si and glass surfaces an array of identical arbitrary-shape atomic nanostructures with the minimum size of an individual nanostructure's element down to 50 nm. Limitations of the approach for fabrication of metamaterials are discovered.

© 2009 Published by Elsevier B.V.

PACS: 03.75.Be; 81.16.Rf; 81.16.Nd

Keywords: Atom nanolithography; Atom optics; Metamaterials

1. Introduction

There is a rising interest in design and discover of metamaterials [1–3]. In the optical frequency range metamaterials could be made on the basis of artificially created atomic and molecular structures on the surface, with characteristic size of individual structure element in nanometer range [3]. At present, the most developed method for surface nanostructure creation is optical photolithography [4]. Photolithography, or exposure of light on a photosensitive material through a photomask, is a widespread technique used to replicate patterns. It is highly developed and well-suited for applications in microelectronics [5]. Today, photolithography

makes possible nanostructures with minimum lateral dimensions down to 45 nm. It is, however, limited to photosensitive materials and is suitable only for fabrication on planar surfaces. Another problem is that in all conventional optical techniques the resolution is restricted by diffraction. When in the path of the light there is an aperture smaller than approximately one half of its wavelength λ , diffraction occurs. In the context of lithography, this means that unlimited reduction of structure size is not possible in mask-based processes: when a gap in a mask becomes comparable with $\lambda/2$, the contours of resulting structures will no longer be clearly defined because of the diffraction effect. Utilization of light sources with shorter wavelengths solves the problem, but makes the method more complicated and expensive. Besides, the light with short wavelengths imposes physical limitations on materials for optical elements (lenses, mirrors, phase masks, etc.).

* Corresponding author.

E-mail address: melentiev@isan.troitsk.ru (P.N. Melentiev).

48 Nanolithographic methods, based on the use of
49 material-particles optics instead of light optics, enables
50 the problem of diffraction limit to be solved, because for
51 most of the particles de Broglie wavelength is essentially
52 less than 1 nm. At present, nanolithography based on uti-
53 lization of focused beams of charged particles (electrons
54 or ions) is best developed [6]. Use of neutral particles
55 instead of charged ones for nanolithography offers few
56 side benefits. Firstly, the lack of charge removes the prob-
57 lem of Coulomb repulsion. Secondly, low kinetic energy
58 of atoms allows to create nanostructures on a substrate
59 without destruction of its surface, what in turn makes it
60 possible to use as substrates a wider class of surfaces:
61 biomaterials, electric microcircuits, etc. Thirdly, the uti-
62 lization of neutral particles enables to realize the “direct
63 method” of nanolithography: nanostructures are created
64 just from the required material.

65 Nanolithography on the basis of neutral atoms is not
66 so well developed as that using light or charged particles.
67 Different approaches to nanostructure creation based on
68 the effect of surface self-assembly of atoms [7], stencil
69 mask nanolithography [8–10], individual atoms control
70 on a surface through the use of a tunnel microscope
71 [11] are known. The above-listed methods have sev-
72 eral restrictions on material, form and linear dimensions
73 reproduction accuracy of nanostructures to be created.

74 An alternative for neutral particles nanolithogra-
75 phy is atom optics [12–15]. During past 10–15 years,
76 atom optics has developed into an important subfield
77 of atomic, molecular and optical physics, and con-
78 tributes to different areas of technology [13]. One of
79 the important trends in atom optics is development of
80 basic elements, which are similar to familiar devices of
81 conventional light optics, such as atom lenses, mirrors,
82 beam splitters and interferometers, as well as application
83 of these elements in practical devices. Among many pos-
84 sible applications of atom–optical elements, a potentially
85 important one is micro- and nanofabrication of material
86 structures, usually referred to as atom lithography [13].
87 In the method, internal and external atomic degrees of
88 freedom are controlled with a very high precision by
89 external electromagnetic fields (or material structures)
90 and thus results in high-resolution surface patterning.
91 Methods of atom lithography are founded on deposi-
92 tion of atoms from a beam sharply focused by an atom
93 lens, generated by a spatially inhomogeneous field of
94 laser radiation [16,17]. Despite numerous suggestions
95 and experimental studies in atom beam focusing [18],
96 the issue has not been resolved experimentally. The cen-
97 tral problem is generation of an atom–electromagnetic
98 field interaction potential, which in properties would be
99 close to “ideal” lens for atoms: with minimum chromatic

aberration and compensated astigmatism while permit-
ting to focus the atom beam into a spot, diffractionally
limited in space.

Recently new approach for nanostructures creation,
based on the idea of object imaging in atom optics via
atom pinhole camera was demonstrated (APC nano-
lithography) [19,20]. The approach has several important
advantages: (1) it makes possible nanostructures with
typical size down to 30 nm; (2) the nanostructures can
have an arbitrary prearranged shape; (3) size and form of
nanostructures are determined by well-controlled param-
eters.

This research has been the first to analyze the pos-
sibility of use APC nanolithography for creation of
metamaterials.

2. Nanolithography based on atom pinhole camera

In an atom pinhole camera, atoms act as photons in
an optical pinhole camera and therefore the main prin-
ciples of imaging by an atom pinhole are akin to those
used in light optics of a pinhole camera. As is generally
known from light optics, a pinhole camera is capa-
ble of producing high-quality (distortion free and high
resolution) object images. Two major questions should
be answered in constructing particular pinhole camera
model: (1) what is the optimum size of the pinhole to
attain maximum resolution; (2) what resolution in this
case is expected. From qualitative physical considera-
tions it is obvious that, at given distance to the image
plane, a large pinhole does not allow to gain an image
of high quality. On the other hand, with far too small an
aperture the diffraction of atoms also hinders an image
construction. The standard approach to imagery through
the use of pinhole camera is to consider image construc-
tion of a point object at infinity. In this case a plane wave
is incident on a screen with pinhole of radius s and at
distance l (focal length of the pinhole camera) a spot
of radius r_g is generated. When the screen pinhole is
large, the spot presents its geometrical shadow, and the
image radius equals that of the pinhole. As the pinhole
decreases, the image spot must be described by physical
optics and Fresnel (or Fraunhofer) diffraction pattern of
the pinhole. In this case, for a circular pinhole the spot
radius $r_d \approx 0.61\lambda l/s$. Hence the radius R of the image
spot made by pinhole camera is roughly (in the axial
approximation) the sum of the image geometrical radius
 r_g and the radius of the diffraction pattern caused by
the aperture $R = r_g + 0.61\lambda(l/s)$, where l is the distance
between pinhole camera and image plane. The smallest
image is achieved when geometrical optics and theory

of diffraction give the same results, i.e. when the condition $s^2 \approx 0.61\lambda l$ is fulfilled. Closer examination based on theory of diffraction shows that the resolution of a pinhole camera can be even better than the geometrical one. Precise calculations [21] show that the image spot diameter at the optimum distance is three times smaller than the pinhole diameter.

An atom pinhole camera (like an optical pinhole camera) is free from linear distortion aberration. The lack of linear distortion follows from the argument based on Fermat’s principle (for small aperture) and from ray optics treatment (in geometrical approximation). The pinhole camera astigmatism comes about because the pinhole aperture appears as an ellipse when viewed not at right angle. The optimum focal length in one plane then differs from that in the perpendicular plane. An atom pinhole camera is also prone to chromatic aberration. This is evident from the relationship between focal distance and wavelength: $l_{opt} \approx s^2/\lambda_{dB}$. In material-particles optics, for the lenses based on electromagnetic interaction potentials the relationship between chromatic aberration and velocity of particles is quadratic. In an atom pinhole camera by virtue of linear relationship between optimum focal length and velocity of an atom, chromatic aberration is linear with respect to the atom velocity, i.e. for atom pinhole cameras this type of aberration is of lesser importance.

The preceding analysis of atom pinhole camera presupposes an infinitely thin screen. In a real experiment the screen thickness is finite, and at sufficiently small aperture the action of van der Waals forces takes effect in atom’s motion through the pinhole. Trajectories of atom’s motion are changed by the action of attractive forces to the walls of nanopinhole channel. In the paraxial approximation the process can be looked upon as an atom beam being defocused by a diverging lens with focal distance:

$$f_{vdW} \approx -\frac{1}{12} \frac{E_k}{C_3 d} s^5 \quad (1)$$

where C_3 is the van der Waals coefficient, d is the thickness of the screen, E_k is the atom’s kinetic energy. Van der Waals’s interaction does not limit the resolution of an atom pinhole camera when the condition $|f_{vdW}| \gg l$ is fulfilled. This relationship defines the pinhole’s minimum size:

$$s \gg a_{min} = \sqrt[5]{\frac{12C_3 dl}{E_k}} \quad (2)$$

For example, for atoms of Cs and a silicon screen 50 nm thick the minimum pinhole radius $a_{min} \approx 55$ nm, for atoms of He the pinhole radius $a_{min} \approx 1$ nm. The above

consideration of atom pinhole camera’s optics shows, that its realization calls for a nanometer diameter pinhole in a screen of nanometer thickness.

In the paper [20] it was demonstrated that nanolithography with use of atom pinhole camera is possible when optimum distance from the pinhole to the mask falls in the range $L = 1–10$ cm, while $l_{opt} \approx 10–30$ mkm. The “reducing power” of the atom pinhole camera $M = L/l$ in this case is $10^3–10^4$. For this geometry of atom pinhole camera, typical dimensions of the mask lie within the range of micrometers, and typical dimensions of the structures created on a surface—within the range of nanometers; i.e. atom pinhole camera provides a means for transformation of objects with micrometer sizes into objects with nanometer sizes. There is another outcome of the atom pinhole camera “scaling geometry”, especially important for development of metamaterials. It is the possibility to use in one device not a single pinhole, but their large array. In this case each pinhole generates its own image, which does not intersect the neighboring ones, i.e. the realization of an “atom-multiple pinhole camera” (AMPC) is possible.

AMPC nanolithography opens up wide opportunities for simultaneous generation of great numbers nanostructures for metamaterial fabrication: (1) with nanostructures’ position and size disorder, (2) lithography of identical nanostructures arranged on to the substrate surface in the appropriate ordered way. The first case of AMPC nanolithography was reported in [19]. The second one is the main topic of this paper. Two major questions come to mind in this case: (1) how far identical are the nanostructures; (2) does the distance between neighboring nanostructures (spatial period) is the same on the whole substrate surface. Main limitations to the identity of the parameters in AMPC nanolithography could be divided as attributed to: (1) membrane with nanoholes and (2) surface substrate. Let us note that even at significant quantity of pinholes (up to 10 million ones) inclined-beams aberrations (beginning to show up in the outermost pinholes) are not that restrictive for the resolution of an “atom-multiple pinhole camera”. Thus effect of membrane is restricted to technical limitations of production regularly spaced nanoholes with equal diameters and mechanical stability of thick membrane [22]. Example of the effect attributed to the surface substrate and limiting the identity of fabricated nanostructures is atom’s surface diffusion. It is known that the effect leads to gain lateral size of nanostructures created by surface growth approaches [23]. In the case of AMPC nanolithography it opens a problem of identity of the effective atom-surface sticking coefficient throughout the surface substrate.

3. Experimental setup

Layout drawing of the atom pinhole camera realized in this research is shown in Fig. 1(a). Besides the pinhole itself it includes: an atom beam, a mask, a nanoaperture and a substrate on which the nanostructures were created. The atoms having passed through the mask apertures form, by analogy with ray optics, a “luminous object” of prearranged geometry. Parameters of the atom pinhole camera were chosen for reason of gaining camera’s maximum resolution and a possibility to construct large arrays of surface nanostructures: $l \approx 20$ mkm, $L \approx 5$ cm, diameters of nanoholes $d \approx 20$ nm. At the parameters chosen an AMPC was operated near a limit of its resolving power. In this case the impact of both diffraction of de Broglie atom waves on pinhole parameters and van der Waals forces becomes essential.

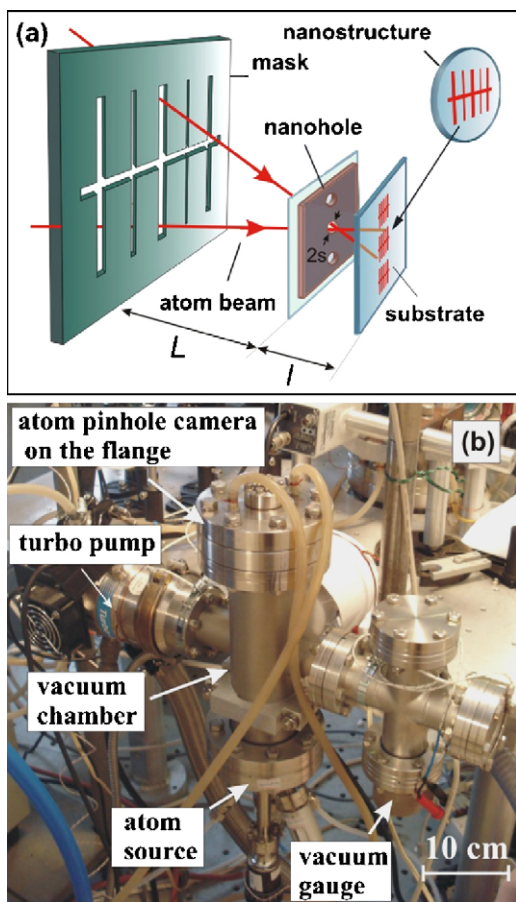


Fig. 1. (a) A schematic drawing of the experiment for nanostructures creation by means of atom pinhole camera. The atoms having passed through the mask apertures form, by analogy with light optics, a “luminous object” of prearranged geometry. An atom nanostructure with the shape of the mask’s scaled down image is generated on the substrate. (b) Photo of the AMPC nanolithography experimental setup.

To produce an array of nanoholes a dual beam column Quanta 200 3D (FEI company) equipped with ELPHY Quantum (Raith company) electronics and software were used for direct ion beam milling suitable to the problem of nanometrous-range holes (up to molecular size) fabrication in a nanometrous-thin membrane produced in a solid [24]. The method enables to make apertures with diameters down to several nanometers [25]. To produce nanoapertures for atom pinhole camera, 40 nm SiO₂ low stress membranes mounted in the center of a cylindrical disc 3 mm in diameter and 0.2 mm thickness (Ted Pella Inc.) have been used (Fig. 2(a)). Important characteristics of the membrane are superior flatness and stability provided by 200 nm Si₃N₄ support mesh. The mesh divides 40 nm thick 0.5 mm × 0.5 mm SiO₂ film on to 24 fields of 50 μm × 50 μm (Fig. 2(b)). The FIB-entry side of the specimen is coated with 10 nm Al in order to prevent charging. Fig. 2(c) shows a SEM image of one of the SiO₂ membrane field with apertures (diameter $d \approx 80$ nm) arranged in staggered rows.

An AMPC with the above parameters has been realized and employed for fabrication of nanostructures made of In, Au and Ag on a silicon and glass surface. AMPC has been placed into a UHV chamber with the after-vapor pressure in the order of 2×10^{-7} mbar (Fig. 1(b)). In the experiments a mask was produced from 40 μm thick metal screen, in which by the method of laser cutting dissimilar-widths through slits was made (Fig. 3(a)). As a source of atomic beam a high temperature effusion cell was used, operated close to the top limit of atomic beam flux applied in the MBE layer growth applications, providing rates of nanostructures growth up to 0.3 Å/s. The generation time for a nanostructures series on one substrate has been determined by atom beam intensity and desired value of nanostructures height. Typical time of exposure in the experiment has been $t \sim 10$ min for nanostructures of height $h \sim 25$ nm. The geometry of nanostructures has been studied by means of atomic force microscope CP-II of the Veeco company.

4. Experimental results

Fig. 3(b) shows AFM image of single nanostructure of In atoms on silicon surface created by the atom pinhole camera with the use of nanoapertures of diameter $d \approx 20$ nm. The presented image shows that form of the nanostructure topologically copies the mask: an individual nanostructure consists of parallel dissimilar-widths stripes crossed by separate stripe, built up from atoms of

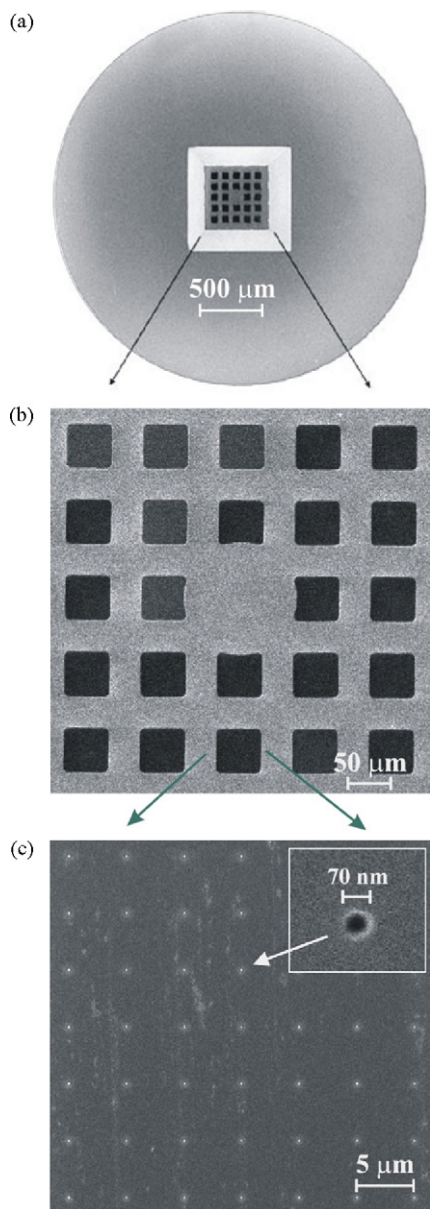


Fig. 2. (a) Photo of membrane with holder in the form of a disc 3 mm in diameter and 200 μm in thickness for the atom pinhole camera. (b) SEM image of 40 nm thick membrane divided by 200 nm thick Si_3N_4 support mesh on to 24 fields. (c) SEM image of one of the SiO_2 membrane field with apertures ≈ 70 nm in diameter, manufactured by the method of ion beam milling. In the inset is SEM image of a single nanohole.

In and separated by equal distances of 390 nm. Width of the nanostructure's first stripe from the left is less than should be in accordance with the width of appropriate slit in the mask; this has been caused by the final aperture of the atom beam, the diameter of which at the mask location is less than the mask size. That is to say, the beam

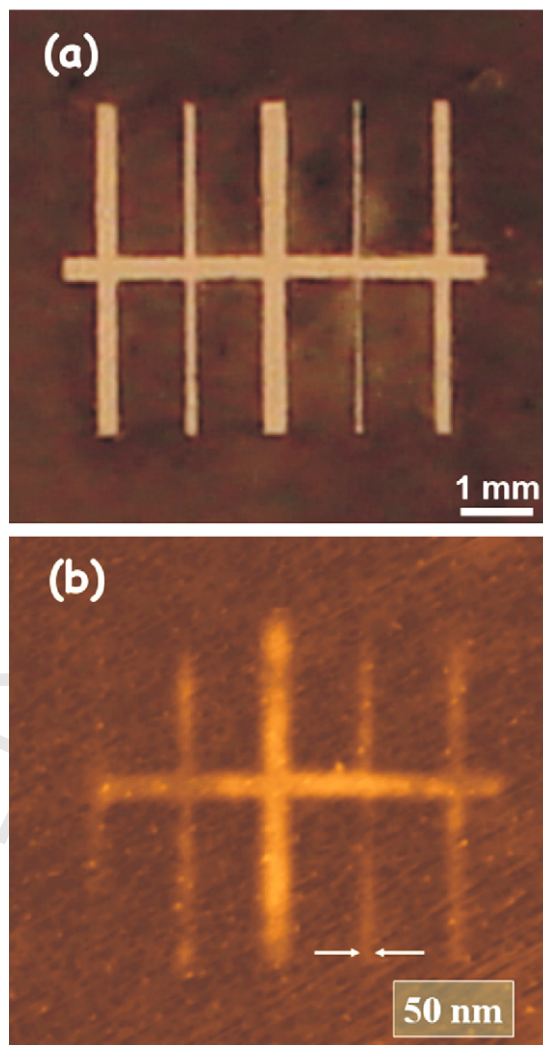


Fig. 3. Atom nanolithography of a single nanostructure: (a) a photo of the mask used; (b) an AFM image of a nanostructure built up from In atoms on a silicon surface.

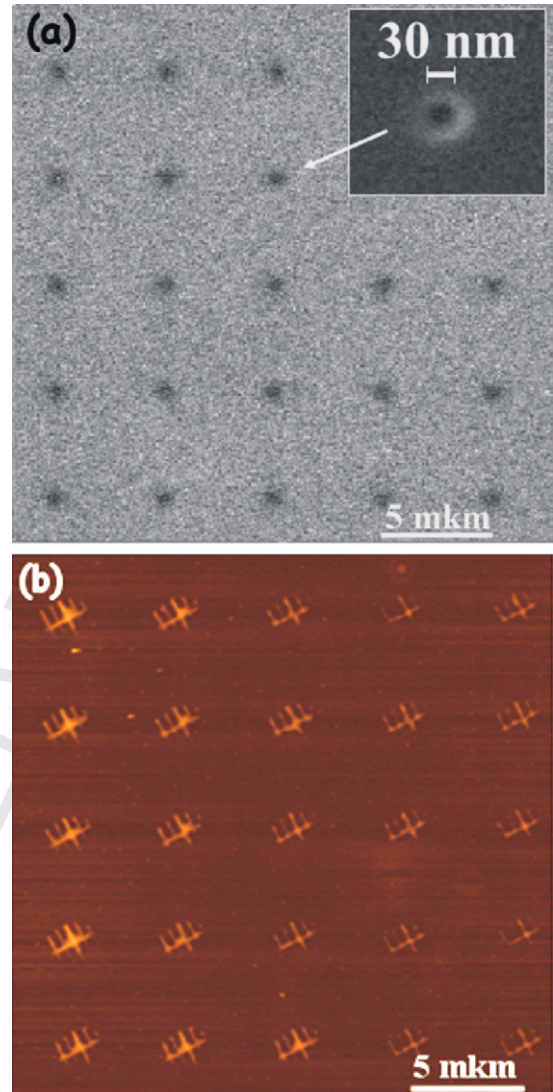
atoms have not passed through full aperture formed by the mask's slits, resulting in curtailment of the stripe length and width. Analysis of the nanostructure's geometrical parameters Fig. 3(b) indicates that the width and height of its constituent strips differ, being determined by widths of the slits in the utilized mask. To the 250 μm slit there corresponds a nanostructure element with the width of $\Delta_1 \approx 120$ nm and the height of $h_1 \approx 7.6$ nm, to the 100 μm slit—an element with the width of $\Delta_2 \approx 80$ nm and the height $h_2 \approx 2.8$ nm. The minimum size of an element, built up in the generated nanostructure from the atoms, that passed through a mask's slit with the width of 40 μm , equals to 50 nm. This value is 18 nm larger than one obtained in a linear atom trajectories analysis of pinhole camera imagery and attributed to effect of van der

336 Waals interaction and atom diffraction on to nanoaperture
337 ure. The height of this element does not exceed the value
338 of 1.8 nm. Non-uniformity of the measured nanostructure
339 's elements in height is determined by various widths
340 of the slits in the utilized mask, which dictates the stream
341 of atoms building up the corresponding element of the
342 nanostructure.

343 Possibility of use APC nanolithography for creation
344 of metamaterials has been investigated in a separate
345 experiment. For this purpose nanostructures have been
346 constructed by means of an atom pinhole camera contain-
347 ing an array of nanoapertures with a period $5\ \mu\text{m}$,
348 see Fig. 4(a). Such an array with holes diameter about
349 30 nm was created in every 24 fields of the SiO_2 film
350 (Fig. 2(b)). Thus whole area occupied by nanostructures
351 was $24 \times 50\ \mu\text{m} \times 50\ \mu\text{m}$. Created nanostructures of In
352 atoms on glass surface are presented in Fig. 4(b). This
353 figure shows that the arrangement of nanostructures on
354 the substrate correlates with that of nanoapertures in the
355 membrane of the AMPC: each nanostructure is formed
356 by atoms having passed through a particular nanoaperture.
357

358 To explore the identity of nanostructures created we
359 have measured dispersion of stripes width for outermost
360 nanostructures on the substrate. It was found that the
361 value is less than 2% and corresponds to the resolution
362 limit of our AFM operated with ultra sharp 1 nm
363 tip. While dispersion of stripes height was measured
364 on the level of 13% and can be attributed to noniden-
365 tity of nanoholes diameter: the height is proportional to
366 intensity of the atom beam near the substructure sur-
367 face which in turn depends on nanoaperture diameter.
368 These measurements show that at chosen parameters of
369 experiment, when the AMPC is operated near a limit of
370 it's resolving power, effect of nanoholes diameter on to
371 nanostructures width is negligible in comparison to it's
372 impact on to nanostructures height. This is direct evi-
373 dence of influence both diffraction of de Broglie atom
374 waves on pinhole parameters and van der Waals forces.
375 Measured value for a dispersion of nanostructure's space
376 period localization on the substrate is appeared to be
377 about 1.6% and is attributed to the thermal drift of the
378 membrane's holder during ion-beam milling procedure.

379 Measured difference of nanohole's diameter is a
380 direct consequence of used technique for fabrication of
381 nanoholes in the membrane. In this method massive ions
382 with energies of thousands electron-volts impinge on a
383 substrate surface and an atomic scale process starts. In
384 this process approximately one atom is removed from the
385 surface for every incident atom thus identity of nanoholes
386 diameter is sensitive to homogeneity of the membrane.
387 Thus the method should be substantially improved to be



388 Fig. 4. Atom nanolithography of identical nanostructures with the use
389 of atom pinhole camera. (a) SEM of membranes with nanoapertures of
390 diameter about 30 nm. In the inset is SEM image of a single nanohole.
391 (b) AFM image of nanostructures built up from In atoms on a glass
392 surface.

393 used in the AMPC nanolithography of identical nanos-
394 tructures.

395 AMPC nanolithography opens up opportunities to
396 build bulk metamaterials by creation of 3D nanostruc-
397 tures. It can be implemented by layer by layer deposition
398 and by controlling height of individual element of each
399 nanostructure. Topology of nanostructure's layers is
400 determined by geometries of an AMPC mask utilized
401 to build these layers.

402 The AMPC nanolithography has several advantages
403 in comparing with currently used e-beam lithography for
404 metamaterials fabrication. First, AMPC nanolithogra-
405

phy is a bottom up approach: the desired nanostructures are created directly from required material. Second, the AMPC has a possibility to produce identical nanostructures in massive parallel way, while in direct writing by a focused e-beam every nanostructure is created one by one. Third, a small atomic kinetic energy opens up a possibility to fulfill lithography on to delicate surfaces without its destruction.

One of the AMPC nanolithography features important for metamaterials fabrication is the possibility to create heterostructures. This comes from the fact that atom pinhole camera imagery weakly depends on sort of material used to produce nanostructures. To build heterostructure composed from two layers of materials “A” and “B” it is necessary to use the pinhole camera with double cell MBE source having possibility to evaporate independently material “A” and material “B”. Successive evaporation of these materials through the AMPC’s mask and a pinhole leads to formation of heterostructures. This approach can be extended to production of heterostructures consisting of layers of multiple materials. There are two basic limitations of the approach: the technical one—clogging of the AMPC’s pinhole that reduces number of possible layers of a heterostructures, and the physical one—when AMPC is operated close to its ultimate resolution limit difference of physical properties of evaporated materials (mainly the de Broglie wavelength and the atom-surface van der Waals potential) leads to different focal lengths of the AMPC thus planar dimensions of a heterostructure’s layers attributed to different sort of materials become nonidentical.

5. Conclusion

The above results demonstrate a possibility to generate identical nanostructures on a silicon and glass surfaces by means of an AMPC. Forms and sizes of the nanostructures created in this approach are governed by the topology of utilized masks and the size of nanoapertures in the membranes. In the process it is conceivable to control not only planar dimensions of the nanostructure’s elements, but also their height. This circumstance is essential for generation of nanostructures with complicated 3D geometry: the form of nanostructures is defined by the arrangement of apertures forming the mask, while the height of individual elements of nanostructures—by the diameter of these apertures.

We will point out that the method of nanostructures creation presented in this research falls in the category of nanolithographic mask-using ones. In the known methods of lithography, mask elements for nanostructures creation must have dimensions in a nanometrous range

and hence their fabrication is a complicated problem both technologically and fundamentally. One advantage of atom pinhole camera utilization for nanolithographic purposes is its feature to generate images with gigantic reduction of the object size—down to 10 thousand times. This makes it possible to use masks of a micrometrous range of dimensions, and their production presents no big problems.

In conclusion, we have successfully implemented the concept of atom pinhole camera as a novel tool for fabrication of metamaterials offering the following merits: (1) it makes possible nanostructures with typical size down to 50 nm; (2) the nanostructures can have an arbitrary prearranged shape; (3) size and form of nanostructures are determined by well-controlled parameters; (4) creation of the great number of identical nanostructures is possible; (5) a variety of materials for nanostructures (atoms, molecules and clusters) is feasible; (6) the method is free from use of a chemically selective etching; (7) in the process of nanostructures creation no destruction of the substrate surface happens.

Acknowledgements

The authors express their thanks for assistance in organization and carrying out of the experiment, as well as discussion of the research results to O.N. Kompanets, E.A. Vinogradov, A.E. Afanasiev. The work has been performed with partial support of the RFBR grants 08-02-12045, 08-02-00871, 08-02-00653 and 09-02-01022.

References

- [1] V.G. Veselago, The electrodynamics of substances with simultaneously negative values of ϵ and μ , *Usp. Fiz. Nauk* 92 (1967) 517–526.
- [2] D.R. Smith, J.B. Pendry, M.C.K. Wiltshire, *Metamaterials and negative refractive index*, *Science* 305 (2004) 788–792.
- [3] A.K. Sarychev, V.M. Shalaev, *Electrodynamics of Metamaterials*, World Scientific, Singapore, 2007.
- [4] C.A. Mack, *Fundamental Principles of Optical Lithography*, John Wiley and Sons, London, 2007.
- [5] M.J. Madou, *Fundamentals of Microfabrication*, 2nd ed., CRC Press, Boca Raton, 1997.
- [6] Y. Chen, A. Pepin, *Nanofabrication: conventional and nonconventional methods*, *Electrophoresis* 22 (2001) 187–207.
- [7] B.D. Terris, T. Thomson, *J. Phys. D: Appl. Phys.* 38 (2005) 199.
- [8] M. Kreis, F. Lison, D. Haubrich, D. Meschede, S. Nowak, T. Pfau, J. Mlynek, *Appl. Phys. B* 63 (1996) 649–652.
- [9] R. Lüthi, R.R. Schlittler, J. Brugger, P. Vettiger, M.E. Welland, J.K. Gimzewski, *Appl. Phys. Lett.* 75 (1999) 1314.
- [10] J. Arcamone, M.A.F. van den Boogaart, F. Serra-Graells, J. Fraxedas, J. Brugger, F. Pérez-Murano, *Nanotechnology* 19 (2008) 305302.
- [11] D.M. Eigler, E.K. Schweizer, *Nature* 344 (1990) 524–526.

- 501 [12] V.I. Balykin, V.S. Letokhov, *Atom Optics with Laser Light*, Har- 515
502 wood Acad. Publ., Chur, 1995. 516
- 503 [13] V.I. Balykin, V.V. Klimov, V.S. Letokhov, *Handbook of The- 517*
504 oretical and Computational Nanotechnology, 7th ed., Elsevier, 518
505 Amsterdam, 2006. 519
- 506 [14] P. Meystre, *Atom Optics*, Springer-Verlag, New York, 2001. 520
- 507 [15] M. Mützel, M. Müller, D. Haubrich, D. Rasbach, D. Meschede, 521
508 *Appl. Phys. B* 80 (2005) 941. 522
- 509 [16] V.I. Balykin, V.S. Letokhov, *Opt. Commun.* 64 (1987) 523
510 151–156. 524
- 511 [17] C. Bradley, W. Anderson, J.J. McClelland, R. Celotta, *Appl. Surf. 525*
512 *Sci.* 141 (1999) 210. 526
- 513 [18] J.J. McClelland, *Handbook of Nanostructured Materials and 527*
514 *Nanotechnology*, vol. I, Academic Press, San Diego, 2000, pp. 528
335–385. 529
- [19] V.I. Balykin, P.A. Borisov, V.S. Letokhov, P.N. Melentiev, S.N. 515
Rudnev, A.P. Cherkun, A.P. Akimenko, P.Y. Apel, V.A. Skuratov, 516
JETP Lett. 84 (2006) 466–469. 517
- [20] P.N. Melentiev, A.V. Zablotzkiy, D.A. Lapshin, E.P. Sheshin, A.S. 518
Baturin, V.I. Balykin, *Nanotechnology*, in press. **Q1** 519
- [21] C.F. Meyer, *The Diffraction of Light, X-ray and Material Partic- 520*
cles, Edwards JW, Arbor Ann, Michigan, 1949. 521
- [22] M. Boogaart MAF, L.M. Lishchynska, J.C. Doeswijk, J. Greer, 522
Brugger, Sens. Actuators A 130–131 (2005) 568–574. 523
- [23] E. Jurdik, H. Rasing Th, C.C. Kempen, J.J. Bradley, McClelland, 524
Phys. Rev. B 60 (1999) 3. 525
- [24] D.P. Adams, M.J. Vasile, V. Hodges, N. Patterson, *Microsc. 526*
Microanal. 13 (2007) 1512–1513. 527
- [25] J. Li, D. Stein, C. McMullan, D. Branton, M.J. Aziz, J.A. 528
Golovchenko, *Lett. Nat.* 412 (2001) 166–169. 529

UNCORRECTED PROOF